Liquid Crystals
Publication details, including instructions for authors and subscription information:
http://www.informaworld.com/smpp/title~content=t713926090

Phase ordering of the liquid crystalline 'B$_7$' phase by analysis of fractal growth patterns

I. Dierking; H. Sawade; G. Heppke

Online publication date: 06 August 2010

To cite this Article Dierking, I. , Sawade, H. and Heppke, G.(2001) 'Phase ordering of the liquid crystalline 'B$_7$' phase by analysis of fractal growth patterns', Liquid Crystals, 28: 12, 1767 — 1773
To link to this Article: DOI: 10.1080/02678290110067533
URL: http://dx.doi.org/10.1080/02678290110067533

LIQUID CRYSTALS, 2001, VOL. 28, NO. 12, 1767–1773

Phase ordering of the liquid crystalline 'B_7' phase by analysis of fractal growth patterns

I. DIERKING*, H. SAWADE and G. HEPPKE

Ivan-N.-Stranski Institut für Physikalische und Theoretische Chemie,
Technische Universität Berlin, Strasse des 17. Juni 115, D-10623 Berlin, Germany

(*Received 27 January 2001; in final form 13 March 2001; accepted 14 April 2001*)

The phase ordering process of bent-core mesogenic molecules is qualitatively different from that observed for conventional rod-like (calamitic) mesogens. Fractal dimensional analysis can be employed to characterize the phase ordering process of these unconventional mesogens. The phase transition between the isotropic melt and the liquid crystalline 'B_7' phase of a 'banana-molecule' material has been investigated in terms of fractal growth patterns, with respect to sample thickness and rate of temperature change. It is shown, that there is a crossover from confinement dominated phase growth to volume behaviour, while the cooling rate has no influence on the dimension of the fractal patterns observed during the phase ordering process.

1. Introduction

Since the introduction of fractal geometry by Mandelbrot [1], this concept has provided a powerful tool in the description of naturally formed complex structures in all areas of science. These areas range from physics and chemistry (growth patterns, aggregation, surfaces and interfaces, viscous fingering, electrochemical deposition) to material science (fracture, dielectric breakdown), biology (growth of bacterial colonies, retina nerve cells) and geology (coastlines, earthquakes) [1–4]. From the fractal dimension of growth patterns, conclusions may be drawn relating to the nature of the ordering process. In the model of diffusion limited aggregation, a fractal dimension in the order $D = 1.7$ is predicted, and this is often verified in aggregation processes of colloids. Percolation systems in a two-dimensional medium on the other hand exhibit a fractal dimension $D = 1.56$ below, $D = 1.89$ at and $D = 2$ above the percolation threshold. These two models account for a large number of growth processes observed in condensed matter systems [1–4].

For conventional calamitic liquid crystals, the phase ordering process from the isotropic melt is generally observed as a nucleation and growth process, obeying universal scaling laws [5–9], in agreement with theoretical predictions for condensed matter systems [10]. The observed structural elements, spherical nematic or cholesteric domains and smectic bâtonnets, are not fractal, exhibiting an euclidean dimension of $D = 2$. This situation is different for unconventionally shaped mesogenic molecules. As pointed out in [11], discotic liquid crystalline phases may grow with a dendritic-type texture, which exhibits a non-euclidian, fractal dimension.

Also bent-core mesogens, or so called 'banana liquid crystals' [12], have been shown to exhibit fractal growth patterns of the B_2 phase [13, 14], formed in quenching experiments from the isotropic melt. The presently reported investigations on the phase ordering of the 'B_7' phase are somewhat different. Here, phase ordering is accomplished from a line-like, spiral filament growth with a dimension $D = 1$ to a space-filling structure of dimension $D = 2$. The phase ordering process from filaments to space-filling textures via filament growth and aggregation can be monitored by the evolution of the fractal dimension of the growth structures. Investigations were carried out with particular focus on variation of sample thickness (liquid crystal cell gap, confinement) and different cooling rates. Attention was also paid to the process of filament formation and growth immediately below the transition from the isotropic melt to the liquid crystal.

2. Experimental

The bent-core mesogen used in the present investigations has the following structural formula:

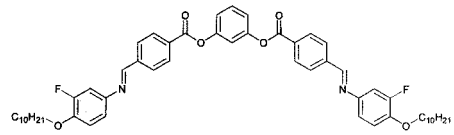

*Author for correspondence. Present address: Institut für Physikalische Chemie, TU Darmstadt, Petersenstr. 20, D-64287 Darmstadt, Germany; e-mail: dierking@hrz2.hrz.tu-darmstadt.de

Liquid Crystals ISSN 0267-8292 print/ISSN 1366-5855 online © 2001 Taylor & Francis Ltd
http://www.tandf.co.uk/journals
DOI: 10.1080/02678290110067533

Its phase sequence on heating, as reported in [15] from DSC measurements, is given by: Cr 119 'B_7' 159 I (°C). Transition temperatures on cooling are shifted a few degrees to lower temperatures, as also indicated in the DSC curves of [15]. They coincide with the temperatures observed in this study by microscopy on samples of thick cells. Here, we are concerned only with the transition from the isotropic to the liquid crystalline 'B_7' phase. The temperature of this transition is dependent on sample thickness, as shown in figure 1, with the transition temperature T_C taken on slow cooling with a rate $R = -0.2\ \mathrm{K\ min^{-1}}$, at the observation of the first liquid crystalline filaments growing into the isotropic melt. Interestingly, the transition temperature is lower for small cell gaps, while one would intuitively expect an increasing transition temperature with decreasing cell gap, due to the ordering influence of the substrates. For cells of gap $d > 6\,\mu\mathrm{m}$, T_C is basically constant (figure 1).

The phase ordering process was followed by use of a Leitz Laborlux 12POLS polarizing microscope, equipped with a Mettler FP82 hot stage and a FP80 temperature controller for relative temperatures better than 0.1 K. Textures were recorded with a Hitachi KP-C551 CCD camera in combination with frame grabber software (MIRO-television). The image size was 768×576 pixels, corresponding to a sample area of $870 \times 650\ \mu\mathrm{m}^2$.

Fractal image analysis was carried out with BENOIT 1.3 (Trusoft-International) using three different methods. First is the *box dimension method*, which defines the fractal dimension D_b from the exponent in the proportionality

$$N(d) \sim \frac{1}{d^{D_b}} \qquad (1)$$

with $N(d)$ being the number of boxes of size d being occupied by the data set. The evaluation procedure is as follows: a grid of boxes with side length d is placed over the object to be analysed and the number of occupied boxes N is determined. Here, every box which contains at least one pixel of the object is counted. This procedure is carried out for a variety of different box sizes and N is plotted as a function of d in a double logarithmic graph, figure 2 (*a*). The dimension D is then determined from the slope of the linear regime of $N(d)$ by minimization of the standard deviation. The object is euclidian if $D = 1$, i.e. it represents a smooth line in

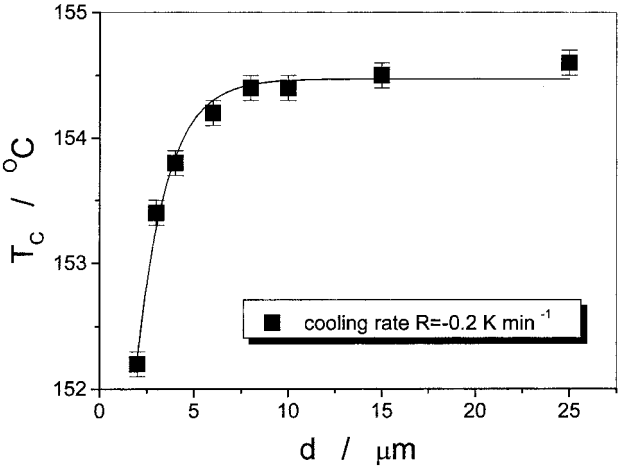

Figure 1. Dependence of the isotropic to liquid crystalline 'B_7' phase transition temperature T_C on sample thickness, while slowly cooling at a rate $R = -0.2\ \mathrm{K\ min^{-1}}$. Transition temperatures were taken on first observation of spiral liquid crystal filaments by polarizing optical microscopy.

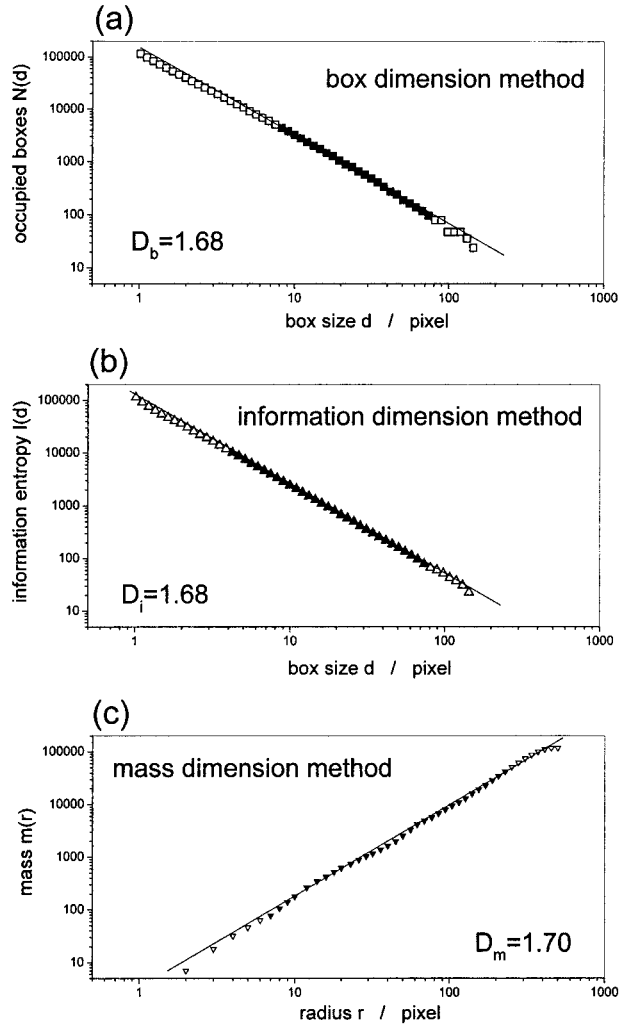

Figure 2. An example of data obtained for the fractal analysis of a texture of a $d = 4\,\mu\mathrm{m}$ sample at $T_C - T = 0.6$ K (■: box dimension method, ▲: information dimension method and ▼: mass dimension method). The fractal dimensions were evaluated from the linear regime of the curves by minimization of the standard deviation to $SD < 0.001$ (closed symbols). Data points for small and large box/radius dimensions (open symbols) were disregarded in the evaluation.

two dimensional space. Also if $D = 2$, the object is euclidian; a smooth plane in two-dimensional space. If in two-dimensional space on the other hand we have $1 < D < 2$, then the object is fractal.

Second is the *information dimension method*, where the fractal dimension D_i is obtained from the proportionality

$$I(d) \sim -D_i \log(d) \tag{2}$$

with $I(d)$ being the information entropy of $N(d)$ boxes of size d, defined by

$$I(d) = -\sum_{i=1}^{N(d)} m_i \log(m_i) \tag{3}$$

with $m_i = M_i/M$, where M_i is the number of points in the i-th box and M the number of total points in the data set. This method is quite similar to the box dimension method, as it follows the same basic procedure. But in contrast to the box dimension method, the information dimension method assigns a weight to the occupied boxes according to the number of object pixels they contain. Boxes with a larger number of object pixels count more than those with less points.

Thirdly, the *mass dimension method* yields the fractal dimension D_m from the proportionality

$$m(r) \sim r^{D_m} \tag{4}$$

with $m(r) = M(r)/M$ the 'mass' within a circle of radius r, where $M(r)$ is the number of data set points contained within a circle and M the total number of points in the set. The evaluation proceeds as follows: a circle of radius r is placed over the object to be analysed and the number of object pixels $M(r)$ within the circle is determined. A mass $m(r)$ is then assigned to the circle of radius r by division of $M(r)$ by the total number of pixels M. This procedure is repeated for a variety of different radii and $m(r)$ plotted in a double logarithmic graph, figure 2 (*c*). From the slope of the linear regime of the curve obtained, the fractal dimension is determined by minimization of the standard deviation. All three methods should give comparable dimensions.

Figure 2 depicts an illustrative example of typical data obtained by the methods applied to the texture observed for a 4 μm cell at 0.6 K below the clearing point. The fractal dimension was in each case determined by minimization of the standard deviation of a linear fit to a log–log plot according to equations (1), (2) and (4) to $SD < 0.001$. For each procedure, the box/radius size was varied over more than two orders of magnitude, resulting in a variation of the dependent variable over about four orders of magnitude. The linear regime, from which the fractal dimensions were determined, covered at least one decade in box/radius size and within the limits of error one finds $D_b \approx D_i \approx D_m \approx 1.69$. All fractal dimensions D given below represent an average of values determined by the three methods employed and their error is estimated to ± 0.02.

The dependence of phase ordering of the liquid crystalline 'B_7' phase from the isotropic melt on sample dimension was investigated at various cell gaps between 2 and 25 μm at a constant cooling rate of $R = 0.2$ K min^{-1}. For all investigations, commercial liquid crystal test cells from E.H.C. (Japan) were used, with a parallel rubbed polyimide orientation layer (generally promoting planar alignment conditions for calamitic mesogens). The dependence on cooling rate R was investigated at constant cell gap of $d = 2$ μm. The filament width was determined from images of size 350×260 μm^2 with a software zoom option set to 400%.

3. Results and discussion

It has been shown before [15–17], that the 'banana "B_7" phase' exhibits a line-like filament growth of spiral structures on cooling from the isotropic melt, figure 3 (*a*). On further cooling, this is accompanied by formation of liquid crystalline aggregates, figure 3 (*c*), which are qualitatively different from those observed in nucleation and growth processes for calamitic liquid crystals. Conventional liquid crystals generally exhibit a phase ordering process which proceeds via nucleation and, under appropriate anchoring conditions, spherical domain growth. This is not the case for phases of bent-core mesogens. These also form at arbitrary nucleation sites, but grow into non-conventional patterns, either in branched or irregular aggregates as for B_2 phases [13, 14], resembling percolation clusters with a fractal dimension of the order $D = 1.85$, or starting in filament growth and subsequent aggregation as for 'B_7'. The irregularity and complexity of the observed growth patterns suggest an analysis by fractal geometry.

Figure 3 shows a series of examples of textures for the growth process of the 'B_7' phase (bright) from the isotropic melt (black) for a $d = 4$ μm cell at a cooling rate of $R = -0.2$ K min^{-1}: (*a*) $T_C - T = 0.15$ K, a spiral filament of euclidean dimension $D = 1$, (*b*)–(*e*) filaments and aggregates with increasing fractal dimension $1 < D < 2$ at $T_C - T = 0.3$, 0.45, 0.75 and 1.25 K, respectively, and (*f*) the space filling texture, naturally of euclidean dimension $D = 2$, at $T_C - T = 2.5$ K. The corresponding temperature dependence of the fractal dimension D during the phase ordering process is shown in figure 4 (*a*) for selected cell gaps d. Starting at a dimension $D = 1$ (filament growth), the growth of aggregates is indicated by an increasing fractal dimension until saturation at $D = 2$ for the space filling texture. This saturation value is reached much faster, i.e. closer to the transition temperature, for thick cells as compared with thin ones. For cell gaps of approximately $d > 6$ μm, the influence

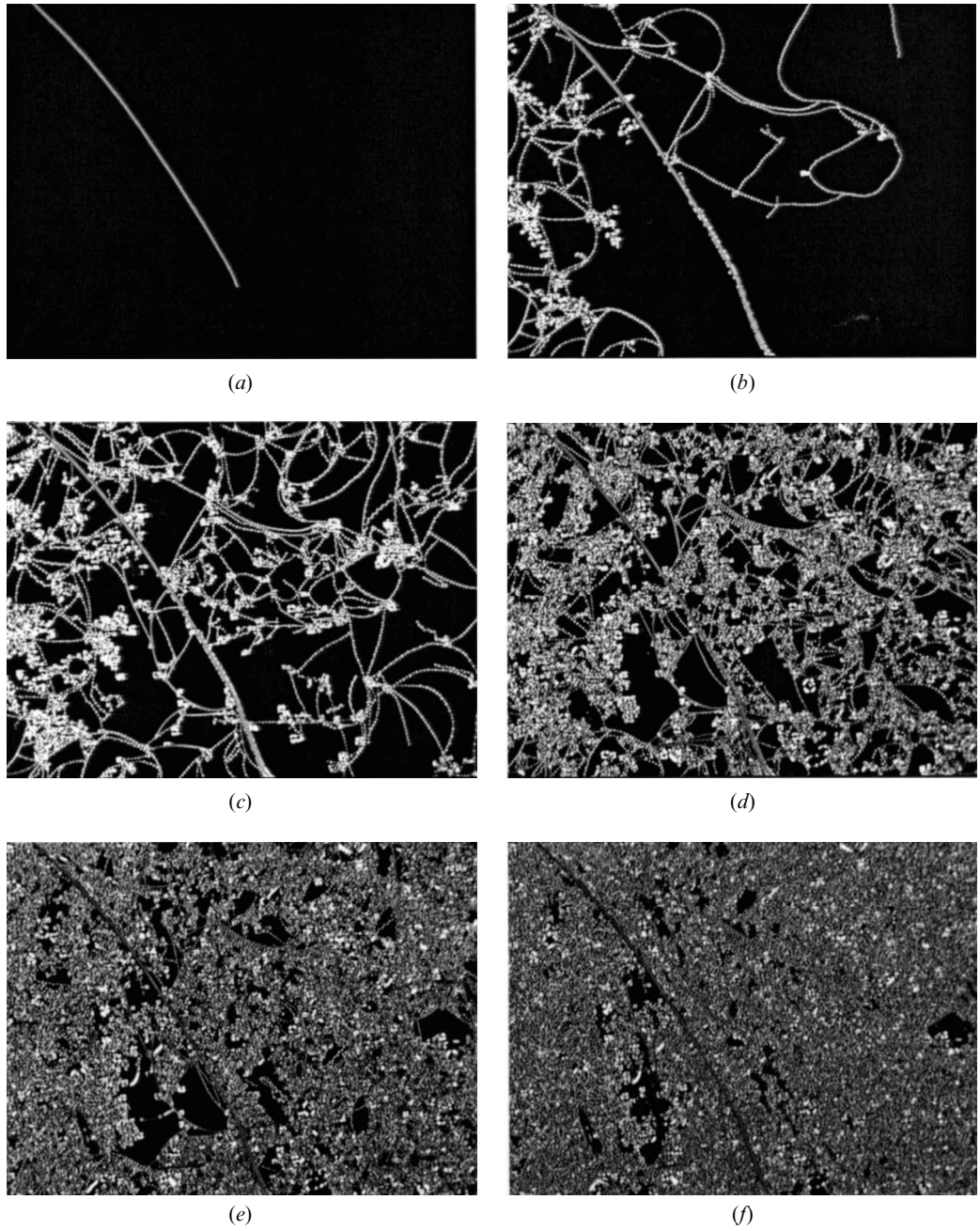

Figure 3. Illustration of the phase ordering process of the 'B_7' phase (bright) from the isotropic melt (black) on slow cooling, $R = -0.2$ K min^{-1}: spiral filament growth at $T_c - T =$ (*a*) 0.15 K, (*b*) 0.3 K, (**c**) 0.45 K, (*d*) 0.75 K, (*e*) 1.25 K and (*f*) 2.5 K. The cell gap of the sample is $d = 4\,\mu$m; each image size is $870 \times 650\,\mu$m^2.

of the confining substrates on the phase ordering process vanishes and the temperature dependence of the fractal dimension is independent of cell gap. For cell gaps $d = 6\,\mu$m and smaller, an influence of confinement on the temperature dependence of the fractal dimension, and therefore also on the phase ordering process, can be observed. At constant reduced temperature, increasingly dense structures are observed with increasing cell gap, as reflected by their fractal dimension and depicted in figure 4 (*b*) as a function of cell gap for some selected reduced temperatures.

Figure 5 (*a*) shows the reduced temperature dependence of the fractal dimension during the phase ordering process for various cooling rates R. All measured D

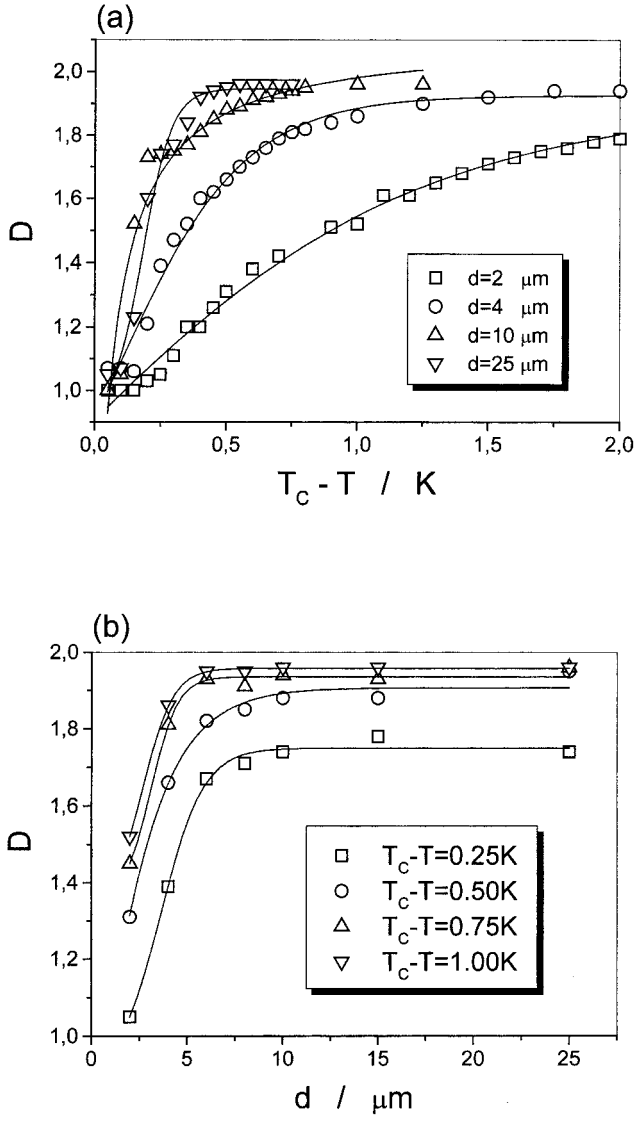

Figure 4. (*a*) Dependence of the fractal dimension D of 'B_7' growth structures on reduced temperature $T_C - T$ for cells of various thickness d. (*b*) Cell gap dependence of the fractal dimension D of liquid crystalline 'B_7' growth structures at selected reduced temperatures $T_C - T$. For cells of gap $d < 6\,\mu m$ a strong influence of confinement can be observed, while for large cell gaps the material behaves in a bulk-like way.

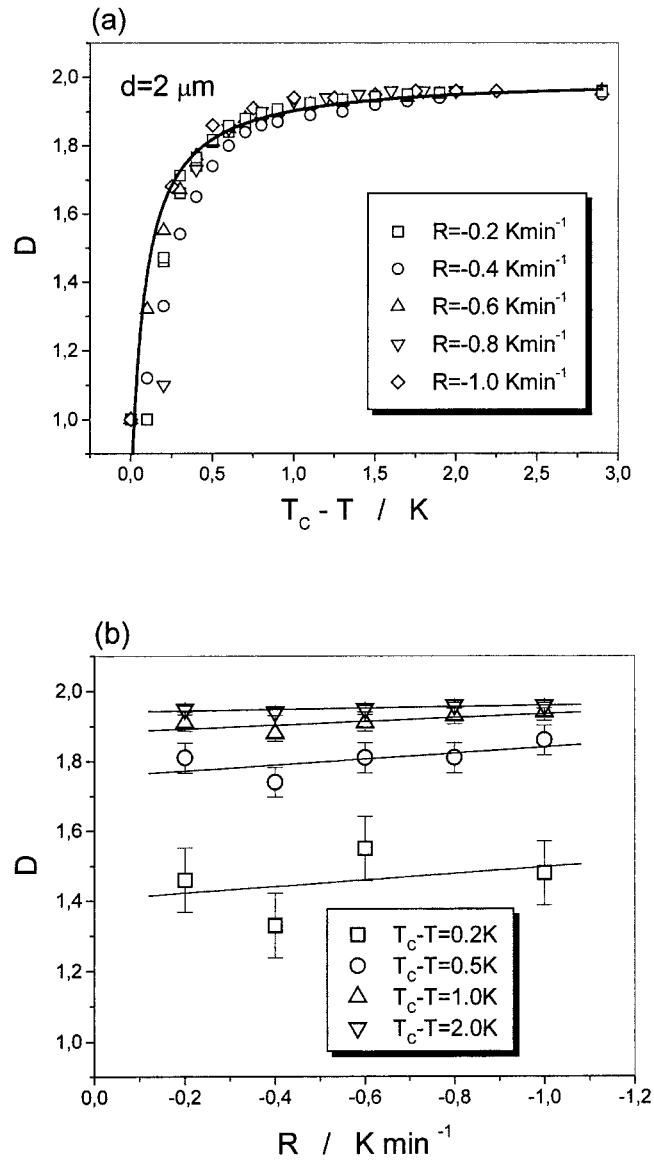

Figure 5. (*a*) Reduced temperature dependence of the fractal dimension D of 'B_7' growth structures for selected cooling rates R. D versus $(T_C - T)$ for all cooling rates can well be described by a single curve (solid line). (*b*) Dependence of the fractal dimension D on cooling rate R. Within the limits of experimental error, D is independent of the rate of temperature variation.

versus $(T_C - T)$ curves are basically equivalent and can be described by a single master-curve. This is more illustratively demonstrated in figure 5(*b*), showing the fractal dimension D as a function of cooling rate at various reduced temperatures. Within the limit of experimental error, the fractal dimension D is independent of the rate of sample cooling. The observed behaviour may be interpreted by the percolation model, crossing the percolation threshold at about 1 K below the clearing temperature.

As mentioned above, the 'B_7' phase ordering process immediately below the transition temperature T_C, is observed as a filament growth of spirals. These can be single spirals, resembling the structure of a telephone cord [15], or double spirals, like an over-twisted telephone cord, figure 6. For small cell gaps $d < 6\,\mu m$, only single spirals were observed, with a spiral width W equal to the cell gap, $W = d$. For cell gaps $d > 6\,\mu m$, single and double spirals appear, with the width of the spirals being independent of the cell gap, and with $W \approx 4\,\mu m$ for single

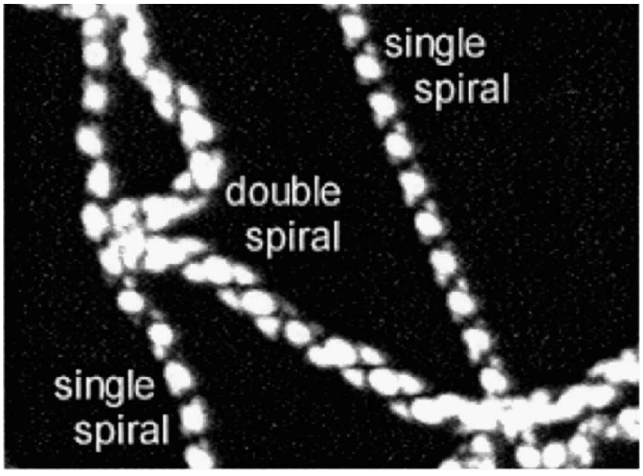

Figure 6. Polarizing microscopic image of spiral filaments in a $d = 10\,\mu m$ cell, close to T_C, illustrating single and double spiral filaments. The image size is $100 \times 75\,\mu m^2$.

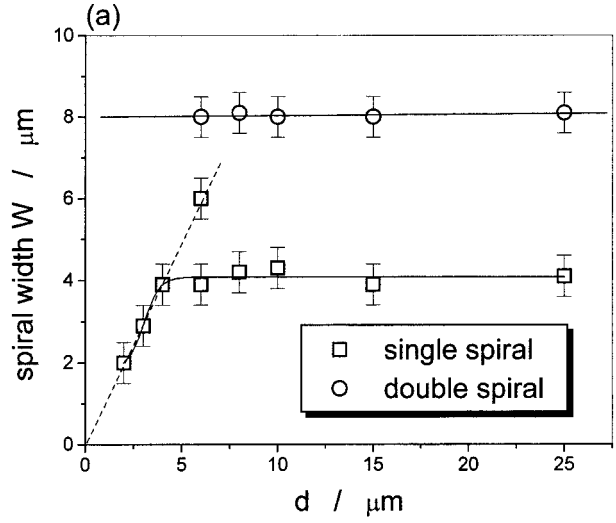

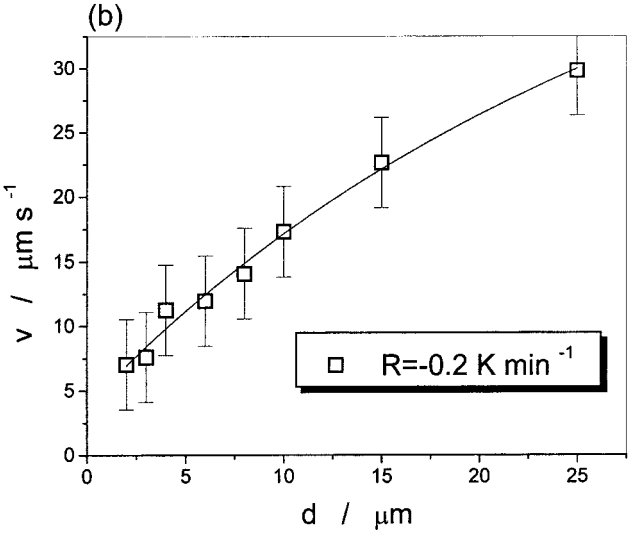

Figure 7. (*a*) Dependence of the width W of single and double spirals on cell gap d, in the early stages of the phase ordering process, close to the transition temperature T_C. The dashed line represents $W = d$. (*b*) Growth velocity v of spiral filaments as a function of cell gap d at a constant cooling rate of $R = 0.2\ K\ min^{-1}$.

spirals and $W \approx 8\,\mu m$ for double spirals, figure 7 (*a*). Again, this clearly indicates the above-mentioned influence of confinement on the 'B_7' phase ordering process for thin cells. Note, that the dimension of $d \approx 6\,\mu m$ determined for the crossover from confinement-influenced to bulk behaviour corresponds well to that determined from fractal analysis of the growth patterns, as well as to the cell gap influencing transition temperatures. The growth velocity v of spiral filaments at a constant cooling rate $R = 0.2\ K\ min^{-1}$ was found basically to increase linearly with cell gap, figure 7 (*b*).

4. Conclusions

The phase ordering process of the 'B_7' phase of a bent core, so-called 'banana-mesogen' was investigated by means of fractal dimensional analysis. Molecules of a bent-core structure do not exhibit regular nucleus growth as observed for conventional calamitic liquid crystal materials, but rather form branched or irregular aggregates, which can be described by a fractal growth process.

Starting at an euclidian dimension of $D = 1$ for first filaments of the 'B_7' phase forming in the isotropic melt, the fractal dimension of the liquid crystalline aggregates increases until at temperatures well below the phase transition temperature, a space-filling texture with again a euclidian dimension, $D = 2$, is obtained. For small cell gaps $d < 6\,\mu m$, the phase ordering process is strongly influenced by confinement conditions, as reflected in the temperature dependence of the fractal dimension. At larger cell gaps of approximately $d > 6\,\mu m$, the material behaves in a bulk-like way, with the temperature dependence of the fractal dimension of the aggregates being independent of sample spacing. The phase ordering process at the I–'B_7' transition is basically independent of cooling rate. Spiral filament growth close to the transition temperature also indicates a crossover behaviour from confinement dominated to volume phase formation.

Note added at proof:

Recently, it was found that the here reported 'B_7' phase might not be structurally equivalent to other B_7 phases reported in [12], although it displays the equivalent textural appearance. Preliminary X-ray experiments suggest that the 'B_7' phase might also be a novel phase or a variant of the B_2 phase with a B_7 texture appearance

(G. Pelzl, S. Diele, W. Weissflog, private communication). This is however at this point not of direct relevance to the reported results, as these are concerned with macroscopic growth patterns rather than microscopic phase structure.

This work was financially supported by the Deutsche Forschungsgemeinschaft and the Fonds der Chemischen Industrie.

References

[1] Mandelbrot, B., 1982, *The Fractal Geometry of Nature* (San Francisco: Freeman).
[2] Vicsek, T., 1989, *Fractal Growth Phenomena* (Singapore: World Scientific).
[3] Bunde, A., and Havlin S. (editors), 1994, *Fractals in Science* (Berlin: Springer Verlag).
[4] Bunde, A., and Havlin, S. (editors), 1996, *Fractals and Disordered Systems*, 2nd Edn (Berlin: Springer Verlag).
[5] Demikhov, E., Stegemeyer, H., and Blümel, T., 1994, *Phys. Rev. E*, **49,** R4787.
[6] Diekmann, K., Schumacher, M., and Stegemeyer, H., 1998, *Liq. Cryst*., **25,** 349.
[7] Dierking, I., 2000, *J. Phys.: Condens. Matter*, **12,** 8035.
[8] Dierking, I., 2000, *J. Phys. Chem. B*, **104,** 10 642.
[9] Dierking, I., 2001, *Appl. Phys. A*, **72,** 307.
[10] Bray, A. Y., 1994, *Adv. Phys*., **43,** 357.
[11] Baehr, C., Ebert, M., Frick, G., and Wendorff, J. H., 1990, *Liq. Cryst*., **7,** 601.
[12] For a recent review on liquid crystalline bent-core molecules see: Pelzl, G., Diele, S., and Weissflog, W., 1999, *Adv. Mater*., **11,** 707.
[13] Dierking, I., 2001, *ChemPhysChem*, **2,** 59.
[14] Dierking, I., 2001, *J. Phys.: Condens. Matter*, **13,** 1353.
[15] Heppke, G., Parghi, D. D., and Sawade, H., 2000, *Ferroelectrics*, **243,** 269.
[16] Pelzl, G., Diele, S., Lischka, C., Wirth, I., and Weissflog, W., 1998, *Liq. Cryst*., **26,** 135.
[17] Lee, C. K., and Chien, L. C., 1998, *Liq. Cryst*., **26,** 609.